Second International Symposium on Marine Propulsors
smp'11, Hamburg, Germany, June 2011

Wind Turbine Propulsion of Ships

Eirik Bøckmann[1], **Sverre Steen**[1]

[1]Department of Marine Technology, Norwegian University of Science and Technology (NTNU), Trondheim, Norway

ABSTRACT

In this paper, the benefits and limitations of wind turbine propulsion of ships are discussed. When designing the wind turbine blades for a wind turbine-powered vessel, the objective is not to maximize the power output, but to maximize the net forward force. The net forward force is the forward force from the water propeller minus the backward force on the wind turbine. This objective results in a different blade design than that of modern commercial horizontal-axis wind turbines. A blade element theory approach to the design of optimal blades for wind turbine powered boats and vehicles is used to design a wind turbine for auxiliary propulsion of a 150 m long tanker. The optimized blade design is shown to result in a higher fuel saving for the ship, when sailing a given route at 10 knots, than what is attained with a commercial wind turbine of the same rotor diameter onboard the ship. Finally, the same ship is equipped with wingsails instead of a wind turbine for auxiliary propulsion, in order to compare the fuel savings. It is seen that the fuel saving is slightly higher when employing the optimally designed wind turbine than when employing wingsails of equivalent sail area as the wind turbine rotor disk area.

Keywords

Wind turbine; wingsail; ship propulsion; blade element theory; fuel saving.

1 INTRODUCTION

Increasing focus on reduction of CO_2 emissions and the possibility of future severe shortage of oil have spurred renewed interest in wind as supplementary propulsion of merchant ships. Several alternative solutions have been considered, like kites, conventional soft sails, rigid sails, Flettner rotors, and wind turbines. A tempting aspect of wind turbine propulsion is that it can provide propulsive force when sailing directly upwind, something that is impossible with the other mentioned forms of wind-assisted propulsion.

In the last decades, vertically oriented airfoils, known as wingsails, have at an increasing rate replaced soft sails as they are aerodynamically more efficient when a high lift-to-drag ratio is important. Indeed, the winner of the 33rd America's Cup (2010), BMW Oracle Racing's trimaran, USA-17, was fitted with a 68 m high rigid wingsail, replacing the traditional soft main sail. Wingsails have also successfully been fitted on several commercial ships for auxiliary propulsion. A recent summary of this is given by Bose (2008). Shukla and Ghosh (2009) estimated the fuel saving for a wingsail-equipped ship sailing Mumbai - Durban - Mumbai at 7 knots to be 8.3%. As far as the authors are aware of, no merchant ships have yet been equipped with a wind turbine for propulsive power generation. One reason for this is that wind turbine propulsion generally provides higher propulsive force than wingsails per turbine/sail area only when the ship speed is less than about half the wind speed (Blackford, 1985). This implies that for wind turbine propulsion to be the preferred form of wind-assisted ship propulsion, a ship cruising at 15 knots must sail an extraordinary windy route with wind speeds above 15 m/s. The other alternative is, of course, to reduce the ship speed, a measure which in itself will reduce fuel consumption.

The height, or air draft, is a limiting factor for both wind turbine ships and ships equipped with soft or rigid sails. The bridges that cross the seaward approaches to the world's major ports restrict the air draft of wind-assisted ships to about 60 m, unless the wind turbine tower, wingsails or masts can be folded down. This means that for a wind turbine-powered ship of length 150 m, the diameter of a non-foldable horizontal-axis wind turbine on deck is limited to about 40 m, considering the freeboard and a safety clearance from the blade tips to the deck. When it comes to stability issues, the increased heel angle due to the wind turbine is shown in this paper to be negligible.

Fig. 1 shows the required propulsive power as a function of ship length for different scalings of a tanker hull at 5, 7.5, 10, and 12.5 knots, as well as the power output from Vestas' wind turbines of varying diameters (The Wind Power, 2010). Hull data for the full scale ship can be found at `http://www.gothenburg2010.org/kvlcc2_gc.html`. The residual resistance for the different ship lengths and speeds is found using Hollenbach's method (Hollenbach, 1998). The transverse projected area above the waterline, A_{TS}, is assumed to be $A_{TS} = 1100\ \mathrm{m}^2 \cdot \left(\frac{L_{WL}\,[\mathrm{m}]}{325.5}\right)^2$, where L_{WL} is the length

of waterline. The corresponding air drag coefficient with respect to A_{TS} is assumed to be $C_{DS} = 0.8$. The required propulsive power is calculated as the total resistance times the ship speed divided by a total efficiency factor of 0.7.

2 OPTIMAL WIND TURBINE DESIGN

2.1 Axial momentum theory

First, let us look at the simple axial momentum theory to see how the task of designing an optimal wind turbine for ship propulsion results in a different blade design than a wind turbine designed to maximize the power output. Consider a wind turbine-powered ship that is sailing at an angle θ' to the apparent wind, see Fig. 2. The true wind direction relative to the ship course is θ. The wind speed is W and the ship speed is u, which together give the apparent wind speed U. From axial momentum theory (Hansen, 2008), the component of the force on the wind turbine parallel to the ship's course is given by

$$F_W = 2\rho_a U^2 a(1-a)A\cos\theta', \tag{1}$$

where ρ_a is the mass density of air, A is the turbine rotor disk area, and a is the axial induction factor. The power generated by the wind turbine is from axial momentum theory

$$P = 2\rho_a U^3 a(1-a)^2 A. \tag{2}$$

The forward force from the water propeller is then

$$F = \frac{P\zeta}{u}, \tag{3}$$

where ζ is the overall propulsive efficiency, which accounts for losses in the power transmission between the wind turbine and the water propeller, as well as water propeller losses. The net forward force, $F_{net} = F - F_W$, then becomes

$$F_{net} = \frac{P\zeta}{u} - 2\rho_a U^2 a(1-a)A\cos\theta'. \tag{4}$$

Inserting Eq. (2) into Eq. (4), and differentiating with respect to a gives

$$\frac{dF_{net}}{da} = 2\rho_a U^2 A\cdot \left[\frac{\zeta U}{u}(1-4a+3a^2) - (1-2a)\cos\theta'\right]. \tag{5}$$

Setting Eq. (5) equal to zero to find a maximum value for F_{net} leads to a quadratic equation which has the solution

$$a = \frac{-(2\cos\theta' - 4\gamma)}{6\gamma} \pm \frac{\sqrt{(2\cos\theta'-4\gamma)^2 - 12\gamma(\gamma-\cos\theta')}}{6\gamma}, \tag{6}$$

where $\gamma = \frac{\zeta U}{u}$. We see from Eq. (6) that if not ζ approaches zero when u approaches zero, $\frac{\zeta}{u}$ will approach infinity, and we cannot use Eqs. (4), (5) or (6). If the ship is sailing directly upwind at half the wind speed and $\zeta = 0.7$, Eq. (6) gives $a = 0.22$, or $a = 0.80$. Momentum theory is not valid for $a > 0.4$ (Hansen, 2008), so the valid solution is $a = 0.22$. If we instead want to maximize the power output from the wind turbine, we differentiate Eq. (2) with respect to a, and set the resulting equation equal to zero. We then find that $a = \frac{1}{3}$ or $a = 1$. Calculating the power coefficient defined as

$$C_P = \frac{P}{\frac{1}{2}\rho_a U^3 A} = 4a(1-a)^2 \tag{7}$$

with $a = \frac{1}{3}$, we get $C_P = 16/27$, which is known as the Betz limit.

Inserting these two values of a gives the results shown in Table 1. We see that although the power from the wind turbine that is optimized for ship propulsion is 10% less, the backward force is 23% less, resulting in a net forward force that is 23% higher than that of the wind turbine that is optimized for power, for the given values of ζ,θ', and $\frac{u}{U}$.

Table 1: Backward thrust, power and net forward force from axial momentum theory.

$\boldsymbol{a}$	$\mathbf{0.22}$	$\mathbf{1/3}$
$F_W/(\rho_a U^2 A)$	0.3423	0.4444
$P/(\rho_a U^3 A)$	0.2673	0.2963
$F_{net}/(\rho_a U^2 A)$	0.2190	0.1778

2.2 Blade element theory

Blackford (1985) showed how classical blade element theory can be used to design optimal wind turbine blades for a wind turbine-powered vessel. Blackford's approach is briefly presented here with the original notation, and applied to design the wind turbine blades for a notional wind turbine ship.

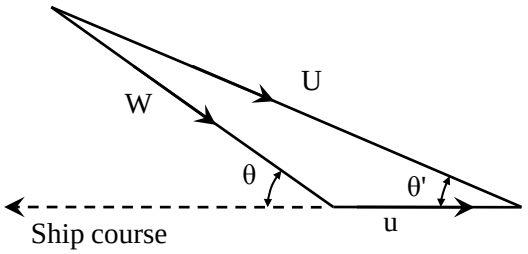

Figure 2: Sketch of wind and ship velocity vectors.

The apparent wind speed, with respect to the wind turbine-powered vessel, see Fig. 2, is given by

$$U = W(1 + f^2 + 2f\cos\theta)^{1/2}, \tag{8}$$

where $f = u/W$ is the ship speed to wind speed ratio. The angle θ', which is the angle between the apparent wind and

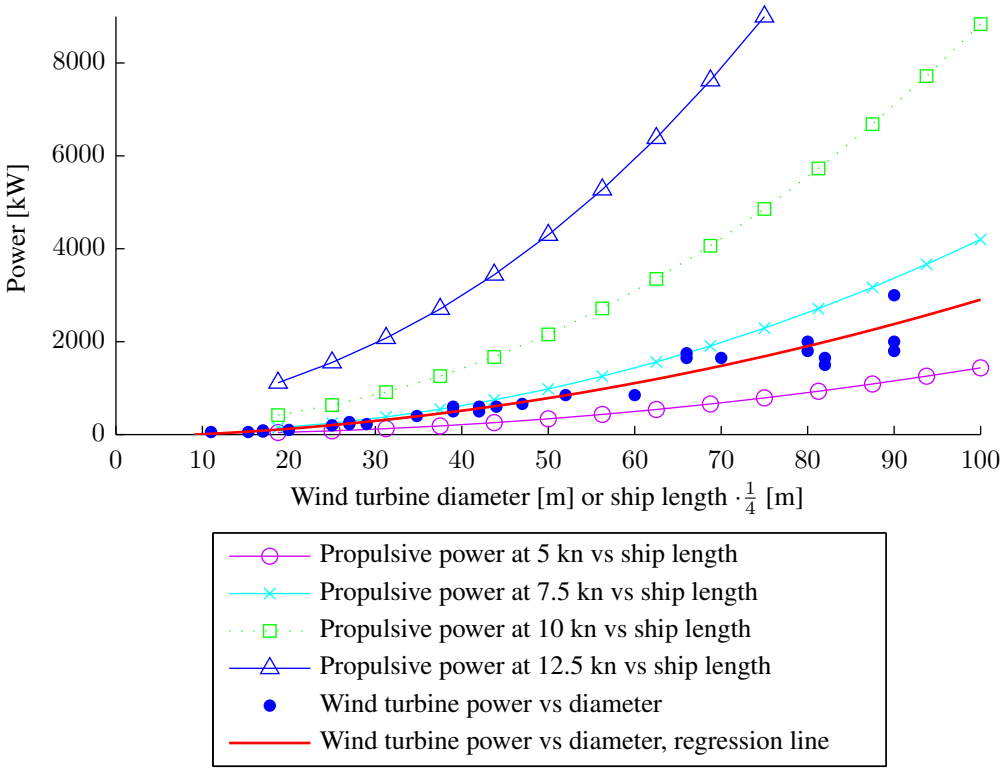

Figure 1: Wind turbine diameter vs power output for Vestas' wind turbines, and ship length vs required propulsive power for scalings of a VLCC hull.

the ship course, is given by

$$\cos\theta' = \pm\left[1 - \left(\frac{W\sin\theta}{U}\right)^2\right]^{1/2}, \qquad (9)$$

where the plus sign is to be used for $0 < \theta' < \pi/2$, and the minus sign for $\pi/2 < \theta' < \pi$. When $\theta' > \pi/2$, F_W is actually helping the ship forward. The apparent wind speed experienced by the rotating blade element at radius r, see Fig. 3, is given by

$$V = ([U(1-a)]^2 + [(1+a')\Omega r]^2)^{1/2}, \qquad (10)$$

where a is the fractional decrease in wind speed when the wind reaches the blade, a' accounts for the induced rotation of the wind field at the blade, and Ω is the wind turbine rotation rate in rad/s.

The power extracted from the wind by the blade element of width dr is given as the product of the tangential component of the aerodynamic force acting on the blade element times the tangential velocity component of the blade element, Ωr, i.e.

$$dP = \frac{1}{2}\rho_a c N V^2 (C_L\sin\phi - C_D\cos\phi)\Omega r dr, \qquad (11)$$

where N is the number of blades, ϕ is the apparent wind angle, c is the chord, and C_L and C_D are the lift and drag

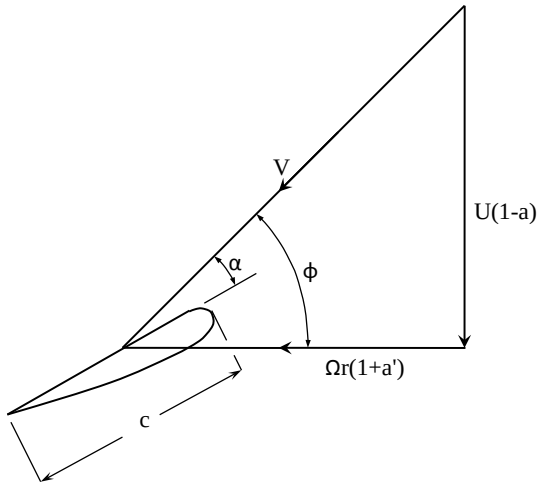

Figure 3: Wind turbine blade element with air velocity components.

coefficients of the blade element respectively. The forward force produced by the water propeller can be derived from the wind turbine power as

$$dF = \zeta dP/u, \qquad (12)$$

where ζ is the overall efficiency factor of the driving mechanism, which consists of all components transmitting the

power between the wind turbine and the water propeller as well as the water propeller itself.

The backward force on the wind turbine will have a component transverse to the motion of the ship as well as parallel to it. Assuming that the transverse force is balanced by a lifting force due to a small leeway angle between the ship and its path, the transverse force component can be ignored. The longitudinal component is given as

$$dF_W = \frac{1}{2}\rho_a c N V^2 (C_L \cos\phi + C_D \sin\phi) dr \cos\theta'. \quad (13)$$

The net forward force, $dF - dF_W$, is found when combining Eqs. (11), (12) and (13) as

$$dF - dF_W = \frac{1}{2}\rho_a c C_L N V^2 \cdot \left[\zeta \frac{\Omega r}{u}(\sin\phi - \epsilon\cos\phi) - (\cos\phi + \epsilon\sin\phi)\cos\theta'\right] dr, \quad (14)$$

where $\epsilon = C_D/C_L$ is the drag-to-lift ratio of the airfoil section. From momentum theory, we know that the backward force on the wind turbine can be written as

$$dF_W = 4\rho_a U^2 a(1-a)\pi r dr \cos\theta'. \quad (15)$$

The power, dP, can be written as

$$dP = \Omega dQ = \frac{1}{2}\rho_a c N V^2 C_L (\sin\phi - \epsilon\cos\phi)\Omega r dr, \quad (16)$$

where the torque, dQ, exerted on the blade elements by the fluid annulus of width dr can from momentum theory be written as

$$dQ = U(1-a)4\pi a' \Omega r^3 \rho_a dr. \quad (17)$$

The alternative expression for dP, $dP = \Omega dQ$, then becomes

$$dP = U(1-a)4\pi a' \Omega^2 r^3 \rho_a dr. \quad (18)$$

Combining Eqs. (12), (18), and (15), the total net forward force can be written as

$$\frac{F_{net}}{4\pi\rho_a R^2 W^2} = \frac{1 + f^2 + 2f\cos\theta}{S^2}\int_0^S a(1-a)H(s)s\,ds, \quad (19)$$

where R is the wind turbine rotor radius, $S = \Omega R/U$ is the tip speed ratio, $s = \Omega r/U$ is the dimensionless speed ratio and the function $H(s)$ is given by

$$H(s) = \zeta\frac{U}{u}\left(\frac{a' s^2}{a}\right) - \cos\theta', \quad (20)$$

where U/u can be obtained from Eq. (8) and $\cos\theta'$ from Eq. (9).

Now, let us keep ζ, f, and ϵ fixed, set $\theta = 0$, and try to maximize F_{net} with respect to $a(s)$ and S. It can be shown (Blackford, 1985) that a' is related to a through

$$a'(s) = -\frac{1}{2}(1 + \epsilon/s) + \frac{1}{2}\sqrt{(1+\epsilon/s)^2 + 4a[(1-a)/s^2 - \epsilon/s]}. \quad (21)$$

Blackford found that the function

$$a(s) \simeq a_0[1 - \exp(-2s)] \quad (22)$$

gives a good approximation for the maximum F_{net} values.

As discussed by Glauert (1943), the maximum velocity reduction in the slipstream, $2Ua$, only occurs on the vortex sheets formed by the trailing vortices from the blade tips. The circumferential average decrease of axial velocity in the slipstream is only a fraction G of this velocity. The wind speed reduction parameter a should therefore be multiplied with G to account for a finite number of blades, N. An approximate expression for G was first worked out by Prandtl, known as Prandtl's tip loss factor:

$$G = \frac{2}{\pi}\arccos\left[\exp\left(-g\right)\right], \quad (23)$$

where

$$g = \frac{N}{2}(1 - s/S)\sqrt{1 + S^2}. \quad (24)$$

The optimal apparent wind angle, ϕ, can be found from

$$\phi(s) = \arctan\left[\frac{1}{s}\left(\frac{1-a}{1+a'}\right)\right], \quad (25)$$

where a and a' are determined from Eq. (22) and Eq. (21) respectively. $\phi(r)$ can be found by substituting $s = \frac{\Omega r}{U}$ into Eq. (25).

By combining Eqs. (13) and (15), we get an expression for the chord length:

$$c = \frac{8\pi U^2 a(1-a)r}{NV^2(C_L\cos\phi + C_D\sin\phi)}. \quad (26)$$

From Fig. 3, we have

$$\sin^2\phi = \frac{U^2(1-a)^2}{V^2}, \quad (27)$$

and by inserting this into Eq. (26), we get

$$c = \frac{8\pi r\sin^2(\phi)a}{N(C_L\cos\phi + C_D\sin\phi)(1-a)}. \quad (28)$$

This is a different expression than what Blackford obtained for c.

3 FUEL SAVING FOR A NOTIONAL WIND TURBINE SHIP

As a result of the considerations discussed above, in the following calculations, a 150 m long ship with the same hull as studied in Fig. 1 is theoretically fitted with a four-bladed 39 m diameter horizontal-axis wind turbine for auxiliary

propulsion, and set to sail the route Peterhead - Bremerhaven - Peterhead, see Fig. 4. This route is chosen primarily due to the weather stations in close proximity to the route, for which statistical wind data is available. The route is divided into 8 legs, where the wind data for each leg is taken from the closest weather station. Table 2 gives the dominant wind directions and average wind speeds for the different legs in January, 10 m above sea level. In order to calculate the wind speeds at an elevation of 39.5 m above sea level, which is the hub height of the notional wind turbine ship, Eq. (29) is used:

$$\bar{U}(z) = \bar{U}_{10} \left(\frac{z}{10} \right)^{\alpha}, \tag{29}$$

where $\bar{U}(z)$ is the mean wind speed at elevation z, $\bar{U}_{10}$ is the mean wind speed at 10 m elevation, and $\alpha = 1/7 = 0.1429$ is a typical value of α (Peterson and Hennessey, 1978).

For given values of θ, W, f, and ζ, there is a value of a_0, see Eq. 22, that gives the maximum possible net forward force for a given wind turbine radius R. In order for the wind turbine to operate at different values of a_0, a different blade design is required for each combination of θ, W, f, if ζ is fixed. This is, of course, totally impractical, and a practical alternative is to use a wind turbine with controllable blade pitch. However, it is not possible to obtain the exact optimal pitch for all radii if the blade is turned a certain angle from, say, the optimal upwind blade pitch. As Blackford points out, it would likely be best to design the wind turbine for optimal performance upwind, since this is the most important and most critical direction. The blades should, nevertheless, be able to be turned in order to optimize the net forward force at different wind directions and wind speeds, and to have full control of the wind turbine and its loads in strong winds.

From the discussion above, the optimized wind turbine ship is designed to sail at 10 kn, with θ = 0 and W = 20 kn = 10.288 m/s, so $f = 0.5$. It is assumed that all blade sections operate at an angle of attack of $\alpha = 4°$, and that $C_L = 0.8$ and $C_D = 0.024$. The chord and pitch angle distributions, see Table 3, are hence fixed, as they are designed for optimal upwind performance, but the blades can be turned, and Ω regulated by a gearing mechanism, to maximize F_{net} for the specific combination of θ, W, and f.

With the chord and pitch angle distributions known, the wind reduction factor, a, is now calculated from Eq. (28). Solving Eq. (28) for a yields

$$a = \frac{b}{1+b}, \tag{30}$$

where

$$b = \frac{cN(C_L \cos\phi + C_D \sin\phi)}{8\pi r \sin^2\phi}. \tag{31}$$

Knowing a, a' is then calculated from Eq. (21). We can now check if the values of a, a' and Ω results in the correct ϕ, see Fig. 3. An iteration procedure must be performed for different angles of attack, α, at each radial blade position, to find the α which gives the correct ϕ. The NACA 4412 foil section is used here, with C_L as a function of α given in Abbott and von Doenhoff (1959). It is assumed that $C_D = \epsilon C_L$, where $\epsilon = 0.03$.

r [m]	ϕ [deg]	c [m]
1	70.8	1.26
3	52.3	3.58
5	40.2	4.30
7	32.1	4.18
9	26.5	3.79
11	22.5	3.34
13	19.6	2.91
15	17.5	2.46
17	16.2	1.93
19	16.0	0.97
19.5	16.9	0

Table 3: Design parameters for the four-bladed optimized wind turbine.

By adjusting the rotation rate Ω and blade angle, for a given blade design, we can get relatively close to the optimal F_{net} if the blades were designed specifically for the actual values of θ, W, and f. F_{net} is found through numerical integration of Eq. (14). The net power in Table 4 is defined as the power generated by the wind turbine minus the power required to overcome the backward force on the wind turbine rotor disk, and can be calculated by multiplying the net force with the ship speed and divide by the efficiency factor ζ_2, which accounts for losses from the engine to the propeller, and propeller losses. With a generator efficiency, $\zeta_1 = 0.95$, the overall efficiency factor then becomes $\zeta = \zeta_1\zeta_2$, and is assumed to be $\zeta = 0.7$ here. The total energy saved using the optimized blade design for θ = 0, W = 10.288 m/s, and $f = 0.5$, when adjusting the wind turbine rotation rate and blade angle, is 40630 kWh. This equals 33.1% of the total required energy, including a sea margin of 15%. A simplified model for the drag on the wind turbine tower is included in the calculations: The tower is divided into two vertical cylinders, one covered by the wind turbine and one uncovered by the wind turbine. The drag force on the tower, $F_{D,t}$, is then calculated as

$$\begin{aligned} F_{D,t} =& C_{D,t} \frac{1}{2} \rho_a \left(U \cos\theta'\right)^2 A_{t,uncovered} \\ &+ C_{D,t} \frac{1}{2} \rho_a \left(U(1-a) \cos\theta'\right)^2 A_{t,covered}, \end{aligned} \tag{32}$$

where $C_{D,t}$ is the drag coefficient of the cylindrical tower, $A_{t,uncovered}$ and $A_{t,covered}$ are the projected areas of the wind turbine tower that are uncovered and covered by the wind turbine, respectively. In the calculations, the following estimated values are used: a = 0.1, $A_{t,uncovered}$ = 30

Figure 4: The route for the wind turbine ship.

m^2, $A_{t,covered}$ = 48.75 m^2 and $C_{D,t}$ = 1.17.

In order to study the effect of optimizing the wind turbine design for a given wind turbine diameter, similar calculations are done for a Vestas V39/600 wind turbine onboard the ship, see Fig. 5. The Vestas V39/600 has a rotor diameter of 39 m, and can generate up to 600 kW of power. Using the power coefficient, Eq. (7), where P is the power found from the power curve (El-Shimy, 2010) for a given wind speed, the axial induction factor, a, is then calculated by solving the cubic equation

$$4a^3 - 8a^2 + 4a - C_P = 0. \tag{33}$$

Note that Eq. (33) has no solution if C_P is above the Betz limit. Solutions of Eq. (33) larger than 0.4 are not valid, due to the limitations of momentum theory. Using axial momentum theory, the component of the force on the wind turbine in the direction of the ship course is given by Eq. (1).

Again, the net force is calculated as the power generated by the wind turbine minus the power required to overcome F_W at 10 knots. As we see from Table 4, employing the Vestas V39/600 wind turbine on the notional wind turbine ship will result in a total energy saving of 24.4% for the given ship and route, compared to 33.1% for the optimized wind turbine design. The drag on the Vestas V39/600 wind turbine tower is set equal to the drag on the optimized wind turbine tower, and again, a sea margin of 15% is used.

Figure 5: Illustration of a Vestas V39/600 wind turbine onboard a tanker for power generation.

4 COMPARISON WITH WINGSAILS

The fuel saving attained for the optimized notional wind turbine ship is compared with that of a notional ship of the same dimensions, using wingsails instead of a wind turbine for auxiliary propulsion. The maximum possible sail area for a particular ship, is

$$SA = K \cdot D^{2/3}, \tag{34}$$

where D is the volume displacement of the ship, and K is a constant, which has the value 3.2 for wingsails (Asker, 1985). Using Eq. (34), the maximum possible sail area for

Leg	Distance	Closest weather station	Dominant wind direction	Average wind speed [m/s] 10 m above sea level
Peterhead - a	63.01 km	Peterhead Harbour	SxSW	6.7
a - b	150.26 km	Forties 3 Platform	SxSW	9.3
b - c	144.97 km	Ekofisk Platform	SxSW	12.9
c -d	140.62 km	Tyra Oest	ExSE	12.9
d - e	118.39 km	Nordseeboje 2	ExSE	9.8
e - f	91.36 km	Feuerschiff Dt. Bucht	N	9.8
f - g	48.15 km	Leuchtturm Alte Weser	SW	10.3
g - Bremerhaven	29.65 km	Bremerhaven	SxSW	6.2

Table 2: Route with wind data for January (Windfinder, 2010).

our ship is 3130.5 m^2. In order to compare the propulsive force for the wingsail-equipped ship with that of the wind turbine-powered ship, a wingsail area equal to the rotor disk area of the wind turbine is chosen. With 10 half-elliptical wingsails of maximum chord length 6.08 m and height 25 m, the total wingsail area is 1194.1 m^2, which is approximately equal to the rotor disk area of the wind turbine, and also well below the limiting maximum possible sail area. It is assumed a 1 m gap between the wingsails and the ship deck, and that this gap is so small that the induced drag is that corresponding to an elliptical wing of half-span equal to the wingsail height. According to Hoerner (1965), this assumption is justified for gaps below 0.06 of the sail height. It is further assumed that the incoming wind is undisturbed by the ship, and that the wind speed at half the wingsail height is representative for the whole wingsail. The wingsail masts are assumed to be 1 m high and 2 m in diameter, which gives a small additional contribution to the total drag.

The wingsail masts are spaced two maximum chord lengths apart, and it is assumed that the local wind at one wingsail is not affected by the other wingsails. This assumption is least incorrect when the apparent wind is abeam. When the wind direction is directly aft, experimental results on groups of longitudinally spaced flat plates normal to the flow (Ball and Cox, 1978) are used to calculate the drag force. It should be noted that the experimental results were obtained at a Reynolds number of $3.9 \cdot 10^3$, while in our case, the Reynolds number based on maximum chord length is up to $6.9 \cdot 10^6$. However, as the drag coefficient for a flat plate normal to the flow is almost constant for a wide range of Reynolds numbers, we believe that it is justifiable to apply these experimental results also for higher Reynolds numbers. The wingsails are assumed to be unaffected by each other until the wind angle is so large that the wingsails begin to shield each other, not accounting for spreading or deflection of the wake, which we consider to be a conservative assumption. From this wind angle, a straight line is drawn down to the drag value for normal flat plates, as shown in Fig. 6.

The wingsails are assumed to have symmetrical cross sections of NACA 0015 profiles. The lift, F_L, and drag, F_D, of the wingsails are calculated as

$$F_L = \frac{1}{2}\rho_a C_L S U^2, \tag{35}$$

$$F_D = \frac{1}{2}\rho_a C_D S U^2, \tag{36}$$

where S is the wingsail area, and the two-dimensional lift and drag coefficients, c_l and c_d, are found from Sheldahl and Klimas (1981) for all angles of attack. Taking the finite span effect into account for the half-elliptical wingsails, the three-dimensional lift and drag coefficients become

$$C_L = \frac{c_l}{1 + \frac{2}{Asp}}, \tag{37}$$

$$C_D = c_d + \frac{C_L^2}{\pi Asp}. \tag{38}$$

The total net forward force for the 10 wingsails, $F_{net,tot}$ is then found as

$$F_{net,tot} = 10(F_L \sin\theta' - F_D \cos\theta'), \tag{39}$$

where the maximum values of $F_{net,tot}$, found by varying the angle of attack, is plotted in Fig. 6. The resulting fuel saving for the wingsail-equipped ship sailing the same route at 10 knots, with a 15% sea margin, is 31.8%.

In order to compare the heeling moments of the wind turbine and wingsail rigs, let us look at the following scenario: The ship is sailing at 10 knots, with true wind direction 104.9° relative to the ship, in 20 m/s true wind speed, so that the apparent wind direction is 90°. The heeling moment due to the optimized wind turbine rig about the center of gravity of the ship is now 6.08 MNm, whereas it is only 1.24 MNm for a Vestas V39/600 onboard the ship. The theory is here applied to get the maximum F_{net} for the optimized wind turbine, which gives both a much larger P and

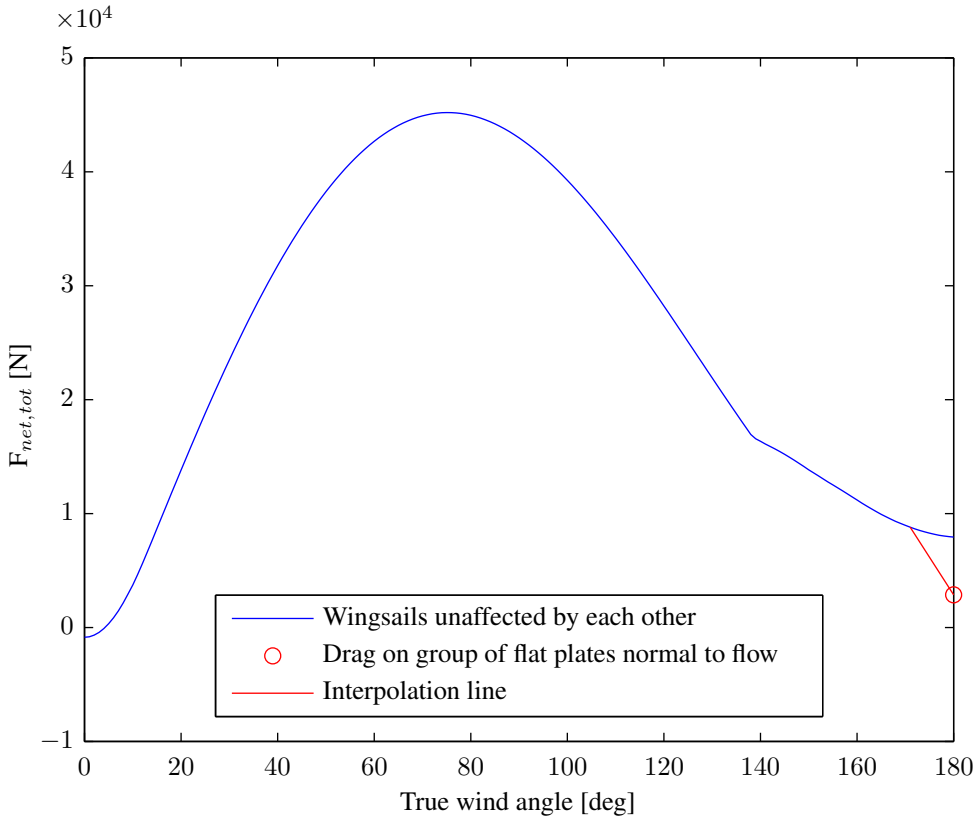

Figure 6: Net forward force from wingsails for a wind speed of 6.7 m/s, 10 m above sea level.

Leg	Net power with optimized wind turbine design for f = 0.5, θ = 0, W = 20 kn [kW]	Net power with Vestas V39/600 [kW]	Net power with wingsails [kW]	Time in leg [h]	Energy saved with optimized wind turbine design for f = 0.5, θ = 0, W = 20 kn [kWh]	Energy saved with Vestas V39/600 [kWh]	Energy saved with wingsails [kWh]
Peterhead - a	107	172	312	3.40	365	584	1060
a - b	325	370	554	8.11	2635	3002	4495
b - c	863	492	1018	7.83	6759	3850	7973
c - d	1195	395	60	7.59	9075	2996	457
d - e	497	343	34	6.39	3179	2191	216
e - f	295	368	417	4.93	1455	1818	2058
f - g	613	355	132	2.60	1594	923	343
g - Bremerhaven	81	134	272	1.60	129	215	435
Bremerhaven - g	69	110	245	1.60	110	175	392
g - f	240	292	397	2.60	624	759	1033
f - e	426	375	573	4.93	2099	1850	2829
e - d	167	215	241	6.39	1068	1375	1543
d - c	560	644	537	7.59	4256	4893	4079
c - b	867	539	958	7.83	6784	4218	7499
b - a	300	362	510	8.11	2435	2941	4139
a - Peterhead	95	144	282	3.40	324	491	959
Sum				**84.93**	**40630**	**30019**	**39023**

Table 4: Energy savings for the ship.

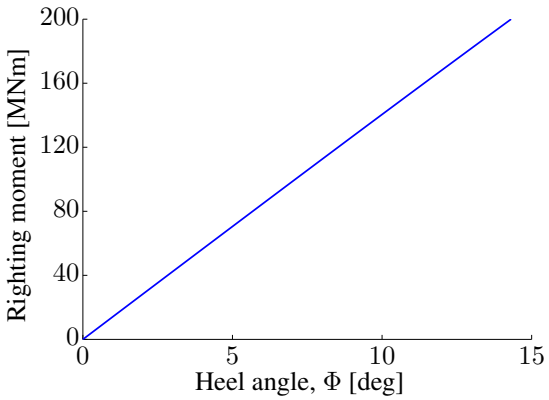

Figure 7: Righting moment for the ship studied.

thrust on the rotor than we get from the Vestas V39/600. This can be seen from the power coefficient, C_P, for the optimized wind turbine, which is 0.3144, whereas the power coefficient for the Vestas V39/600 is only 0.0606 at this wind speed, resulting in a power output of 600 kW. The optimized wind turbine gives a higher net forward thrust than the Vestas V39/600, not because the thrust is lower, but because the power is much higher. This result may seem somewhat counterintuitive since the optimized wind turbine is optimized for maximum F_{net} and not maximum power, but is due to the fact that the optimized wind turbine is designed for higher apparent wind speeds than the Vestas V39/600.

For the same wind condition, the heeling moment of the wingsail rig about the center of gravity of the ship is 4.20 MNm, for a 13.8° angle of attack. An extreme heeling moment may occur if the wingsail rig is positioned to sail upwind, and the wind direction suddenly changes to 20 m/s apparent beam wind, faster the wingsails are turned, so that the angle of attack is 90°. In this case, the heeling moment will be as high as 116 MNm; fortunately only for a short period of time if the wingsail positioning system is working properly. Such large heeling moments will never occur for a wind turbine-powered ship.

The righting moment can be calculated as

$$M_{righting} = \rho_w \nabla g GM \sin\phi, \tag{40}$$

where ρ_w is the mass density of water, ∇ = 30600 m^3 is the volume displacement, GM = 2.63 m is the distance from the center of gravity to the metacenter, and ϕ is the heel angle of the ship. This GM-value accounts for the underwater hull of the ship only. When the righting moment equals the heeling moment, the ship will have a steady heel angle ϕ. The righing moment curve is shown in Fig. 7. We see that for heeling moments below 10 MNm, the heel angle is negligible.

5 CONCLUSION

The 150 m long tanker sailing the route Peterhead - Bremerhaven - Peterhead in January at 10 knots will save 24.4% of the total fuel by employing the Vestas V39/600 for auxiliary power generation. By optimizing the wind turbine design for ship propulsion while keeping the wind turbine diameter fixed at 39 m, the fuel saving increases to 33.1%. Fitting the ship with wingsails of the same sail area as the wind turbine rotor disk area results in a fuel saving of 31.8% at a ship speed of 10 knots. It is seen that the heeling moment in 20 m/s apparent beam wind is lower for a ship powerered by a Vestas V39/600 wind turbine than a wingsail-powered ship, but higher if the ship is powered by the optimized wind turbine described in this paper. However, if one considers the risk of the wingsail turning system failing, a wind turbine-powered ship is preferable with respect to heeling moments. For a ship sailing about half the wind speed, it is thus seen that an optimized wind turbine-powered ship is weakly preferable over a wingsail-powered ship, if energy efficiency and heeling moments are the main concerns.

REFERENCES

Abbott, I. H. and von Doenhoff, A. E. (1959). Theory of Wing Sections. Dover Publications.

Asker, G. C. F. (1985). 'Roller Furled Genoa and Rigid Surface Wingsail, a Flexible Practical Wind-Assist System for Commercial Vessels'. Journal of Wind Engineering and Industrial Aerodynamics, 20:61–81.

Ball, D. J. and Cox, N. J. (1978). 'Hydrodynamic Drag Forces on Groups of Flat Plates'. Journal of the Waterway Port Coastal and Ocean Division, 104(WW2):163–173.

Blackford, B. L. (1985). 'Optimal Blade Design for Windmill Boats and Vehicles'. Journal of Ship Research, 29(2):139 – 149.

Bose, N. (2008). Marine Powering Prediction and Propulsors. SNAME.

El-Shimy, M. (2010). 'Optimal Site Matching of Wind Turbine Generator: Case Study of the Gulf of Suez Region in Egypt'. Renewable Energy, 35(8):1870–1878.

Glauert, H. (1943). Division L of Aerodynamic Theory. Durand Printing Committee, Calif. Institute of Technology.

Hansen, M. O. L. (2008). Aerodynamics of Wind Turbines. Earthscan.

Hoerner, S. F. (1965). Fluid-Dynamic Lift. Hoerner Fluid Dynamics.

Hollenbach, K. U. (1998). 'Estimating Resistance and Propulsion for Single-Screw and Twin-Screw Ships'. Ship Technology Research, 45(2):72–76.

Peterson, E. W. and Hennessey, Jr., J. P. (1978). 'On the Use of Power Laws for Estimates of Wind Power Potential'. Journal of Applied Meteorology, 17:390–394.

Sheldahl, R. E. and Klimas, P. C. (1981). 'Aerodynamic Characteristics of Seven Symmetrical Airfoil Sections Through 180-Degree Angle of Attack for Use in Aerodynamic Analysis of Vertical Axis Wind Turbines'. Technical Report SAND80-2114, Sandia National Laboratories.

Shukla, P. C. and Ghosh, K. (2009). 'Revival of the Modern Wing Sails for the Propulsion of Commercial Ships'. International Journal of Environmental Science and Engineering, 1(2):75–80.

The Wind Power (2010). Wind turbines and windfarms database. http://www.thewindpower.net/manufacturer-datasheet-range-14-vestas.php. Retrieved September 3, 2010.

Windfinder (2010). http://www.windfinder.com. Retrieved August 30, 2010.